

Design and Fabrication of a Nanobiosensor for the Detection of Cell-Free Circulating miRNAs-LncRNAs-mRNAs Triad Grid

Pooja Ratre,^{||} Nazim Nazeer,^{||} Arpit Bhargava, Suresh Thareja, Rajnarayan Tiwari, Vinay Singh Raghuwanshi, and Pradyumna Kumar Mishra*



Cite This: *ACS Omega* 2023, 8, 40677–40684



Read Online

ACCESS |



Metrics & More

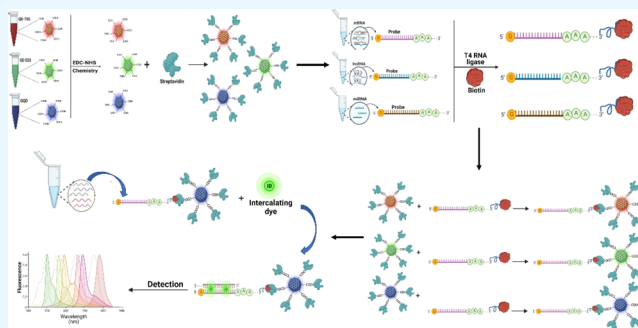


Article Recommendations



Supporting Information

ABSTRACT: The increased understanding of the competitive endogenous RNA (ceRNA) network in the onset and development of breast cancers has suggested their use as promising disease biomarkers. Keeping these RNAs as molecular targets, we designed and developed an optical nanobiosensor for specific detection of the miRNAs-LncRNAs-mRNAs triad grid in circulation. The sensor was formulated using three quantum dots (QDs), i.e., QD-705, QD-525, and GQDs. These QDs were surface-activated and modified with a target-specific probe. The results suggested the significant ability of the developed nanobiosensor to identify target RNAs in both isolated and plasma samples. Apart from the higher specificity and applicability, the assessment of the detection limit showed that the sensor could detect the target up to 1 fg concentration. After appropriate validation, the developed nanobiosensor might prove beneficial to characterizing and detecting aberrant disease-specific cell-free circulating miRNAs-LncRNAs-mRNAs.



INTRODUCTION

The understanding of our genome and associated regulatory processes has increased as a result of the discoveries about the significance of noncoding RNAs (ncRNAs) in physiological and pathological processes. ncRNAs, particularly micro RNAs (miRNAs) and long noncoding RNAs (lncRNAs), are known to have a crucial role in post-transcriptional gene control and cellular functions. Increasing scientific research of ncRNAs has opened up new avenues for investigating the ongoing aberrant mechanisms of different chronic and age-associated diseases and identifying the molecular targets for diagnosis and therapeutics.¹ It is now evident that the aberrant ceRNA network plays a vital role in the onset and progression of several noncommunicable diseases and malignancies, including breast cancer (BC), the primary source of cancer-related complications in women around the world.^{2,3} As per recent estimates, one in every 20 women worldwide and one in eight women in countries with high incomes are affected by BC. Although the average mortality rate from BC has fallen due to the recent developments in therapeutic procedures, early detection and immediate treatment are two crucial factors for the cure of BC.⁴ As the metastatic disease causes more than 90% of BC-related deaths, numerous types of research have been performed to discover new and reliable biomarkers for BC. One of the recently developed biomarkers include ncRNAs such as lncRNAs, miRNAs, and mRNA, which circulates in the human body and has the potential to reflect the different steps of disease development and progression.^{5,6}

These ncRNAs are interrelated and communicate in an intricate way to regulate the expression of vital genes. For instance, lncRNAs have potential miRNA-binding motifs, which can prohibit miRNAs from adhering to their appropriate mRNA targets.⁷ On the contrary, miRNAs can adversely influence the production of lncRNAs by interacting with the corresponding regions. Both miRNAs and lncRNAs can jointly influence the expression of the common mRNAs.⁸ In addition, by interfacing through miRNA regulators or interacting directly with miRNAs, lncRNAs can modify the expression of miRNA target genes, which may regulate the overall gene expression pattern and modulate the ongoing vital cellular processes.⁹ Moreover, such interaction and crosstalk offer new insights into the control of gene expression and disease etiology of aggressive and metastatic BCs. Therefore, it is essential to investigate the lncRNA-, miRNA-, and mRNA-based triple prognostic biomarker assay for early-stage detection of BC.¹⁰

Due to their high sensitivity, simplicity, and cost-effectiveness benefits, optical sensing technologies for detecting different disease-specific biomarkers have gained significant attention. These biosensors utilize the properties of light to identify and

Received: August 4, 2023

Accepted: October 3, 2023

Published: October 18, 2023



Table 1. Primer and Probe Detail Sequences Used for the Profiling

s. no.	primer used	sequences (5'3')
1.	miR-34a – FmiR-34a -R	CAGCTGTGAGTGTCTTTGCTGATTGCTTCCTTAC
2.	ANRIL – FANRIL – R	CAACATCCACCCTGGATCTTAACAAGCTTCGTATCCCCAATGAGATACA
3.	PTEN – FPTEN – R	TGGGCCCTGTACCATCCCAAGTTGTGGCAACCACAGCCATCGT
Uracil-Modified Oligonucleotide Sequence		
	34a – CCGGTCGACACTCACAAAGAAACCGTGAGA	
	ANRIL – GTTGTAGGTGGTGACCTAGAATTGTATCTG	
	PTEN – ACCCGGGACATGGTAGGGTTCAGGAAACAT	

analyze biological substances and biochemical reactions in a given sample.^{11,12} The detection signals rely on the specific interaction between the target analytes and a recognition component immobilized on the sensor's surface. The binding of the target molecule with the recognition element generates optical signals, which quantitatively correlate with the number of analytes present in the sample. These optical sensors are equipped with different light-yielding materials, such as nanomaterials, antibodies, and probes. One of the widely accepted nanomaterials used for optical sensing is quantum dots (QDs).^{13,14}

Compared with other metallic NPs, QDs have enhanced biocompatibility, stable fluorescence characteristics, and limited toxicity, making them preferred moieties for a number of biological applications. In addition, they possess outstanding optoelectric excitation-dependent fluorescent emission, size-tunable optical properties, and photoinduced electron transfer and minimal or no spectral overlap. Due to the important role of RNA in various diseases, exploration of their molecular interaction and transport mechanisms in live cells is highly important in the field of biomedicine. Fewer studies using QD-based electrochemical biosensors as RNA detection tools have been reported in the past few years. For instance, a DNA-mediated silver electrochemical biosensor based on GQDs was reported to have potential applications in detecting microRNAs.¹⁵ Similarly, an analytical electrochemical RNA sensor with a reaction catalyst assisted by horseradish peroxidase was also assessed for detection.¹⁶ However, apart from electrochemical biosensing applications of QDs, the present study investigates the fluorescence aspects of QDs in simultaneous detection of three different RNA classes, i.e., mRNA, lncRNAs, and miRNAs. For this, we designed a specific probe against targeted RNA and assessed a triple sensor using three different-sized and color-based QDs to detect lncRNAs, miRNAs, and mRNAs in biological samples.

MATERIAL AND METHODS

RNA Isolation and Expression Analysis. Cell-free circulating RNAs (lncRNAs and mRNAs) were isolated from the plasma of blood samples using a QIAamp circulating nucleic acid isolation kit (Qiagen, Hilden, Germany) in the described manner (IRB No.: IEC/ICMR-NIREH/ITR-GIA/BC/2022-23/12-01-23). A PCR-based method was used to carry out expression analysis. First, Takara BioInc. PrimeScript first strand cDNA Synthesis kit (Shiga, Japan) synthesized cDNA from the extracted RNAs. The 4 μ L of synthesized cDNA was added to a 10 μ L qPCR Master Mix (Luna universal qPCR master mix, New England Biolabs, Ipswich, Massachusetts, USA). After the addition of specific primers of targeted mRNA (PTEN) and lncRNAs (ANRIL) (Table 1), a PCR reaction was performed on an Insta Q96 Real-Time PCR instrument (Himedia Laboratories, Mumbai, MH, India) under the proper thermal cycling

conditions of the target gene. For the expression analysis' internal control, GAPDH was used. Ct values were acquired, and dCt values were calculated following scheduled PCR cycles.¹⁷

miRNA Isolation and Expression Analysis. A Nucleospin miRNA plasma kit manufactured by Mangeley Nagel (Duren, Germany) was used to isolate miRNAs. The isolated miRNAs were then processed for polyadenylation using the Poly-A tailing kit from Invitrogen-ThermoFischer Scientific in Greenville, NC, USA. The polyadenylated miRNAs were then processed into cDNA synthesis using a cDNA Synthesis kit (Takara BioInc. PrimeScript™ first strand cDNA Synthesis kit, Shiga, Japan), mainly containing oligo-dT primers and reverse transcriptase. The 10 μ L of qPCR Master Mix was then added 4 μ L to cDNA strands with the primers of target miRNAs (34a), and the reaction mixture was placed into a series of amplification cycles on a thermocycler an Insta Q96 Real-Time PCR (Himedia Laboratories, Mumbai, MH, India). U6 was used as an internal control. Ct values were recorded, and dCt values calculated.^{18,19}

Preparation of Triple Sensor. Preparation of Biotinylated Oligonucleotide Probes. Selected complementary uracil-modified oligonucleotide probes for miRNAs, lncRNAs, and mRNAs (34a, ANRIL, and PTEN) were bought from Integrated DNA Technologies (Coralville, Iowa, USA) and attached at the 3' position of biotin by using a Pierce 3'-end biotinylation kit purchased from Thermo Fisher Scientific (Waltham, MA, USA). Briefly, uracil-modified oligonucleotide probes (50 pmol) were incubated for 5 min at 85 °C. Following incubation, probes were swiftly cooled and combined with the appropriate amounts of 10X RNA ligation buffer, biotinylated cytidine (Bis) phosphate, RNase inhibitor, T4 RNA Ligase enzyme, and 30% PEG. The mixture was incubated overnight at 4 °C. After incubation, nuclease-free water (NFW) and chloroform/isoamyl alcohol (in a 24:1 ratio) were added, and high-speed centrifugation was performed to remove the RNA ligase. The resultant layer of water was combined with ice-cold 100% ethanol, glycogen, and 5 M NaCl and incubated to precipitate for 1 h at –20 °C. The obtained pellet was carefully collected and washed with 70% ethanol. The pellet that formed in the next step was resuspended in NFW (20 μ L), set to air-dry, and then kept at –20 °C.²⁰

Preparation of the Streptavidin-Conjugated QDs. Three different QDs, both organic and inorganic types (Qdots S25, QD 705, and GQDs), were procured from ThermoFisher Scientific, Waltham, MA, USA, and Merck KGaA, Darmstadt, Germany. The carboxyl group on the surface of these three QDs was first activated using carbodiimide chemistry comprising EDC (1-ethyl-3-[3-(dimethylamino)propyl] carbodiimide hydrochloride) and NHS (*N*-hydroxysuccinimide) from ThermoFisher Scientific (Waltham, MA, USA). First, an aliquot of QDs was prepared by mixing 10 μ L of each QDs in three different tubes containing 250 μ L of 1× PBS, followed by the addition of 25 μ L of EDC (1 mg/mL solution) and 25 μ L of NHS (1 mg/mL solution) for surface charge activation. The above mixture

was then incubated for 1 h at room temperature (RT). A 100 μL aliquot of streptavidin (1 mg/mL) was added to the previously activated QDs and incubated for 20 min at RT. The activated carboxyl groups on the surface of QDs were then coupled with amine groups of streptavidin via the formation of an amide linkage. To improve the efficacy of the conjugation, a second aliquot of 25 μL of EDC and NHS was added to the tube containing the QDs streptavidin conjugate. This was followed by 1 h of vortexing at RT. Centrifuging at 6000 rpm for 15 min separated the streptavidin coated QDs from the free QDs. The streptavidin coated QDs conjugates were pelleted and stored at 4 $^{\circ}\text{C}$ until further use.

Preparation of Final Nanoconjugates. After streptavidin was bound to the surface of QDs, biotinylated oligonucleotide probes were attached via the streptavidin–biotin coupling reaction to detect targeted miRNAs, lncRNAs, and mRNAs. For conjugation, the Streptavidin-attached QDs were added to 200 μL of 1 \times PBS (pH 7.4), vortexed, and combined with the biotinylated probes in the following ratios: 3:1, 1:1, and 1:3. The reaction mixture was then vortexed for 1 h at RT and incubated overnight at 4 $^{\circ}\text{C}$ for further investigation. The prepared conjugates have target complementary strands on their surface for desired targets (34a, ANRIL, and PTEN) in the isolated sample (Figure 1).²¹

Targeted Detection of miRNA, lncRNA, and mRNA In Biological Samples. Applicability of Developed Triple NanoHybrid. Using fluorometry (Spark multimode microplate reader, TECAN, Seestrasse 103, Mannedorf, Switzerland), we detected three RNA markers in plasma. To achieve this, plasma samples were first filtered through 0.45 μm filters to remove mesenchymal cells and cellular debris such as extracellular micro vesicles, lipid rafts, apoptotic/necrotic bodies, and exosomes and then with 0.22 μm filters to obtain apparent plasma free of any substantial genetic debris. The 10 μL of each nanoconjugate (QDs 705, QDs 525, and GQDs) were mixed with 90 μL of filtered plasma in a microplate reader, followed by addition of different intercalating (propidium iodide and SYBR Safe) dye in each tube, the solution was incubated for 10 min and then analyzed in fluorometry under different channels. The method was repeated for the isolated RNA samples. These samples were examined and compared to a blank solution (NFW), which served as the negative control and did not include any capture or detector components. To assess the repeatability of the nano hybrid, experiments were carried out in triplicate in 15 samples. After the detection applicability assessment of the designed nanoconjugates, the results were validated by performing probe RT-PCR and agarose gel electrophoresis.

Microscopic Evaluation of Developed Triple Sensor. Fluorescence microscopy was used to evaluate the fluorescence properties of prepared nanoconjugates. The nanoconjugates mixed with amplicons of all different targeted RNAs and intercalating dye were added in the same volume as that in the applicability assessment. Different filters according to the excitation and emission of QDs used (FITC, DAPI, and TRITC) were selected. Two fluorescence pictures were uploaded to the ImageJ platform for the colocalization studies. The JaCop plugin was then used to analyze overlapping between the previous two images, which included Pearson's coefficient, overlap coefficient, intensity correlation analysis, Manders' coefficients M1 and M2, and Van Steensel's cross-correlation coefficient.

Selectivity Analysis of the Triple Sensors. The fluorometry method evaluated the prepared conjugates' selectivity toward

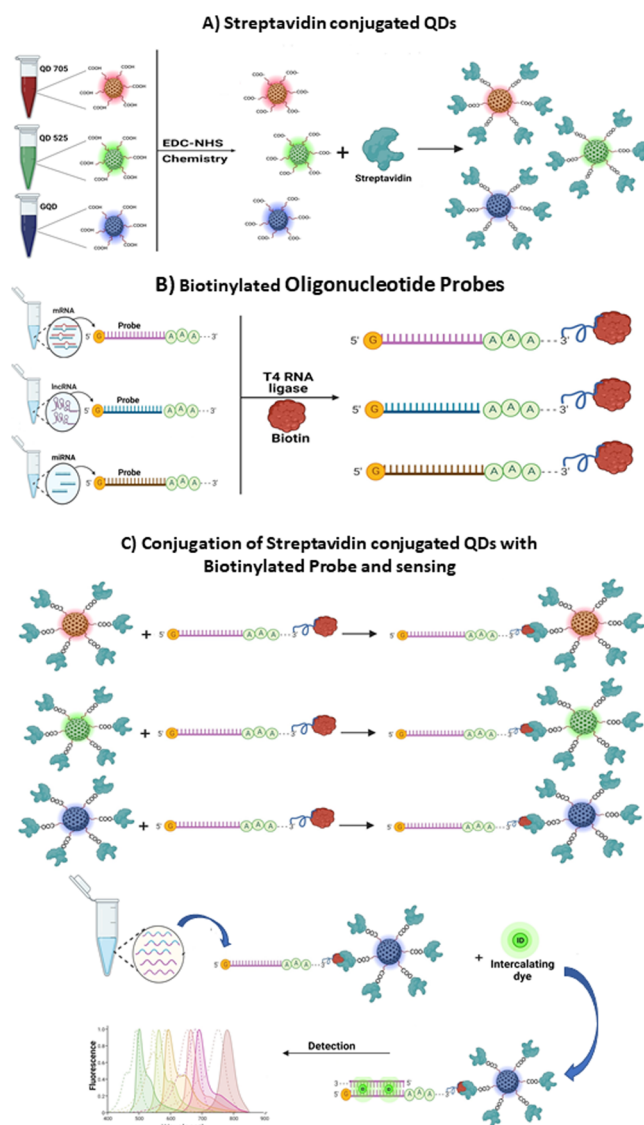


Figure 1. Image showing the fabrication of a triple nano hybrid system (A) showing the preparation of the streptavidin-conjugated with QDs; (B) biotinylation of oligonucleotide probes; (C) conjugation of streptavidin-conjugated QDs with biotinylated probes and sensing.

targeted RNAs. The 10 μL prepared nanoconjugates were mixed in 1 μL of PCR amplicons of the target RNAs (34a, ANRIL, PTEN) and 1 μL of intercalating dye, and the fluorescence intensity was recorded using fluorometry (Spark multimode microplate reader, TECAN, Seestrasse 103, Mannedorf, Switzerland). The nanoconjugates were next tested against PCR amplicons of other nonspecific RNAs (7a, 29a, Gas-5, PVT, PIK3CA, and FOXO3).

Sensitivity Analysis of the Triple Sensors. To check the sensitivity and limit of detection (LOD) of developed nanoconjugates, different dilutions of targeted RNAs amplicons (miRNAs, lncRNAs, and mRNAs), ranging from 1 μg to 1 fg, were prepared in NFW. The 10 μL of prepared nanoconjugates were mixed in 1 μL in 90 μL NFW of all prepared dilutions, and the difference in the fluorescence intensity was recorded using fluorometry (Spark multimode microplate reader, TECAN, Seestrasse 103, Mannedorf, Switzerland).

Statistical Analysis. Each result's mean and standard error were calculated ($n = 3$). The GraphPad Prism Version 5.03 was

used for statistical analysis. One-way or two-way variance analysis was used to calculate the statistical differences.

RESULTS AND DISCUSSION

Biomedical sensing is one of the most promising areas that emerged in the field of nanosensors, as it offers novel methods for rapid and accurate diagnosis of different life-threatening diseases, including BCs. With continuous evolution in molecular biology, various disease-specific biomarkers have been identified. The clinical diagnosis of BCs is now focused on developing novel analytical methods capable of specific and parallel detection of biomarkers.²² The competitive endogenous RNAs (ceRNAs) are essential transcripts that interact with each other to create a regulatory network that is vital for regulating various ongoing biological processes. The interaction between lncRNA-miRNA-mRNA has been suggested to play a significant role in the onset of diseases, including BCs. Substantial investigations have shown that these RNAs' regulatory networks can regulate the oncogenesis process.⁴ Considering this fact, we have developed fluorescent-based triple sensors for the detection of miRNAs, lncRNAs, and mRNAs collectively. The existing methods for detection of these RNAs require additional labeling protocols, amplification techniques, and data normalization processes; however, the method discussed here is simple, specific, and has the ability to perform simultaneous detection of the three triad biomarkers (ccf-miRNA, lncRNAs, and mRNAs) without involving the additional complicated labeling protocols.

Initially, expression profiling of the target RNAs was performed using the qPCR method in 15 samples. The graph shown here represents an upregulated expression of 34a, ANRIL, and PTEN in most samples (Figure 2). Following the

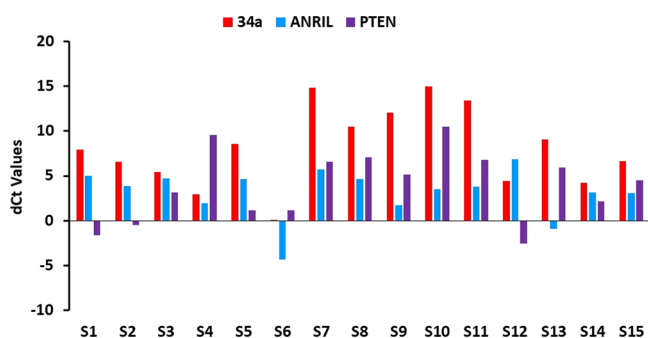


Figure 2. Graph showing the expression pattern of 34a, ANRIL and PTEN targeted RNAs in biological samples through quantitative real-time PCR.

expression analysis, the triple sensor comprising three different QDs (QD-705, QD-525, and GQDs) was designed and assessed for their ability to detect biomarkers (34a, ANRIL, and PTEN) involved in the progression of BC. For the fabrication of the triple sensor, a set of probes highly specific toward target molecules was selected and biotinylated. This was followed by the surface activation of QDs and their subsequent labeling with streptavidin. The three different QDs used showed red (QDs 705), green (QDs 525), and blue (GQDs) color fluorescence with probe-bound mRNA (PTEN), lncRNAs (ANRIL), and miRNA (34a) respectively. The size-dependent spectrum characteristics of the QDs, along with the excellent quantum yield, strong molar extinction coefficient, and broad range of absorption spectrum, uniform fluorescence spectrum, significant Stokes shift, and strong photochemical stability are few of the

unique features of QDs that aid their ability for utilization in sensorics.²³ The selected QDs revealed a polydispersity index of 0.292 (QDs 705), 0.934 (QDs 525), and 0.291 (GQDs) with Z-average values of 1375 187.1, and 390.6 nm, respectively (Figure 3).

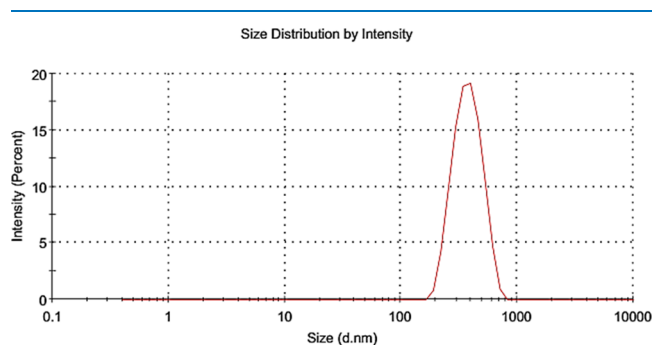


Figure 3. Graph showing the size distribution pattern of QDs.

The binding of the target RNA with the biotinylated probe was determined using intercalating dyes (Sybr safe and propidium iodide). Moreover, the presence of nanoparticle clusters attached to streptavidin and their ability to bind with the target were evaluated using fluorescence microscopy. To confirm their location on the same plain, a merged or colocalized image was taken, which shows in the integrated yellow and green color (Figure 4).

The quantitative change in the fluorescence intensity of functionalized QDs upon binding with the target was analyzed by fluorimetry, which showed that the intensity initially decreases when it binds with streptavidin (Figure 5). This may be due to the phenomenon of fluorescence quenching. In general, it has been shown that the interaction involving the surface atoms of QDs and any molecules or atoms on the surface causes the recombination of electron-hole pairs to be inhibited, which results in fluorescence quenching of QDs. The electron-hole recombination process can be hampered, and changes to the surface or surroundings of QDs can reduce the fluorescence intensity. It is also known that photoinduced electron transfer from an excited QDs to a nearby compound with an energy intermediate to the valence and conduction band edge states causes the fluorescence quenching of QDs and results in a decrease in fluorescence intensity.^{24,25}

The developed nanoconjugates were then analyzed for selective target detection and applicability in filtered plasma samples spiked with target RNA amplicons. The nanoconjugates have oligonucleotide probes on the surface, which are complementary to the targeted miRNA, lncRNA, and mRNA and ensure selective binding. The efficient assimilation of targeted RNAs led to the increased fluorescence intensity of RNA-attached nanoconjugates in contrast to the nanoconjugates attached with streptavidin and probe. Yet, a surge in the fluorescence intensity of intercalating dye was noted, which may be associated with the expression and amount of RNAs present in the plasma sample (Figure 6). The validation of nanoconjugates was performed after detection of target. The PCR results show the amplification of a selected probe against all three targets in different samples. For further confirmation the agarose gel electrophoresis was performed, and the desired bands appeared in the gel images (supplementary Figure 1).

After confirming the applicability of the developed sensor, we further looked for the sensitivity of all three nanoconjugates. The

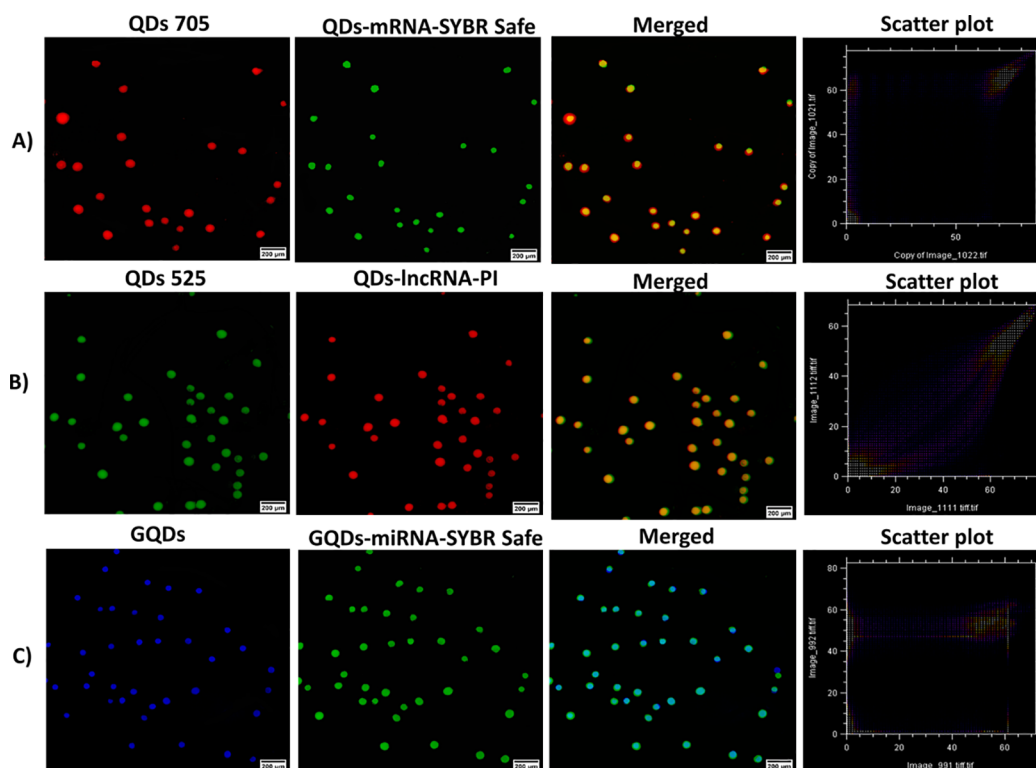


Figure 4. Figure depicting the fluorescence microscopic images evaluation of QDs (A) QDs 705 cluster in red color, green SYBR safe dye confirming the presence of uracil modified probe of mRNA PTEN and merged image of both the images in yellow with colocalized scatter plot. (B) QDs 525 cluster in green color, red PI confirming presence of lncRNAs ANRIL probe, and merged image in yellow with colocalized scatter plot. (C) GQDs cluster in blue color, green SYBR safe dye confirming the presence of miRNA 34a and merged image in blue-green color with colocalized scatter plot.

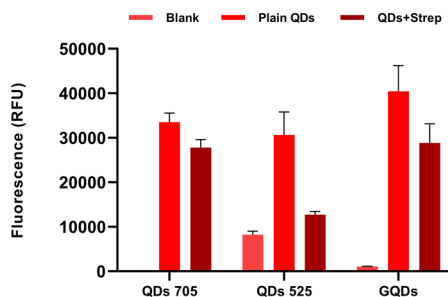


Figure 5. Graph shows the fluorescent comparison analysis of Plain QDs and conjugated QDs in fluorometry.

nanoconjugates were added in different ranges of target RNAs ranging from 1 μ g to 1fg. The results observed via fluorometry, developed nanosensors that can analyze the target up to 1fg concentration and showed the limit of detection (LOD) value of 0.9882 fg (QDs 705), 0.314 fg (QDs 525), and 0.313 fg (GQDs) (Figure 7).

In order to perform specificity assessment, the nanoconjugates were added in the well containing targeted RNA amplicon and with nonspecific RNA amplicons. The fluorescence intensity was highest in the case of the selective RNA amplicon, and low or no fluorescence signal was observed in the nonselective amplicon. The increase in fluorescence intensity on hybridization with specific RNA was observed in all three conjugates due to the fluorescence quenching effect of QDs, and the same increase in fluorescence intensity was observed on addition of intercalating dyes due to their binding with major grooves on nucleotides (Figure 8).

CONCLUSIONS AND TRANSLATIONAL PERSPECTIVE

In today's world of advanced medicine and intelligent healthcare systems, nanotechnology has led to the development of a wide range of laboratory-based tests that have accelerated their broader translational purpose leading to the early detection of noncommunicable diseases such as BC.²⁵ In this scenario, making timely medical decisions based on fast, efficient, reliable, and reproducible diagnostic data has become critical in quality health management and patient care. The increasing use of nanobiosensors will help capture disease-associated marks and provide new insights into signaling events and pathways at the level of both the genome and epigenome. ncRNAs and their interactions have significantly affected BC development, metastasis, and treatment. Different miRNAs, lncRNAs, and mRNAs act alone or in combination on mRNA alone or as competing endogenous RNA (CeRNA) networks for regulation, as they compete for miRNAs at the post-transcriptional stage. Understanding the processes underlying these connections, which impact the expression of genes linked to BC, can help create intelligent analytical techniques for early disease identification. The expanding knowledge about the role of miRNA-lncRNA-mRNA (as a triad grid) in the development and progression of BCs has made them excellent candidates as disease biomarkers. With the rapid growth of QDs in cancer imaging and diagnosis, there has been an increased interest in developing effective cancer diagnostic procedures using these nanomaterials. As we learn more about the significance of ncRNAs and their interactions in BC, we can better understand how to use QDs for early detection. We developed herein a unique triple sensor for the simultaneous assessment of miRNAs-lncRNAs-mRNAs

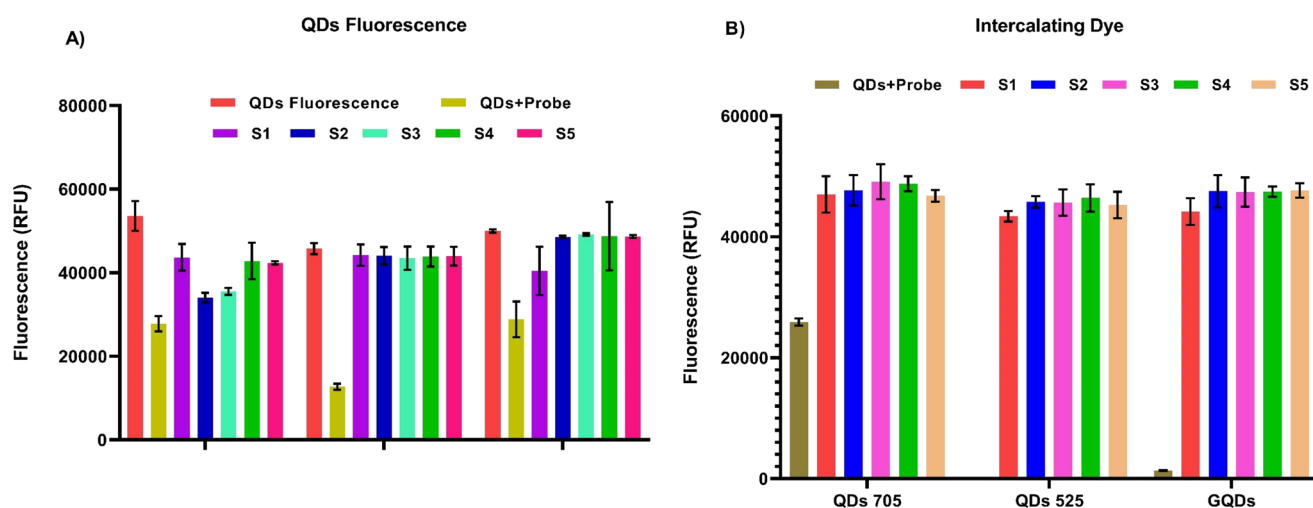


Figure 6. Graph demonstrating the change in fluorescence intensity or applicability of developed nanoconjugates after hybridization with targeted RNAs in fluorometry (A) change in the intensity in case QDs fluorescence (B) change in fluorescence intensity of intercalating dyes.

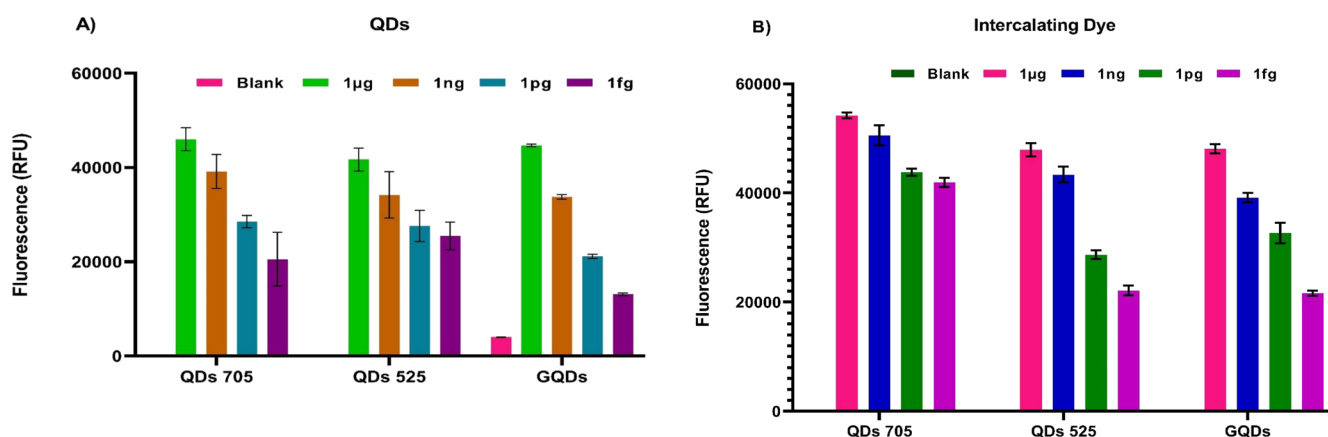


Figure 7. Graph demonstrating the sensitivity of developed nanoconjugates upon hybridization with targeted RNAs in different concentrations (A) Relative fluorescence unit (RFU) of QDs noted in fluorometry (B) RFU of intercalating dyes.

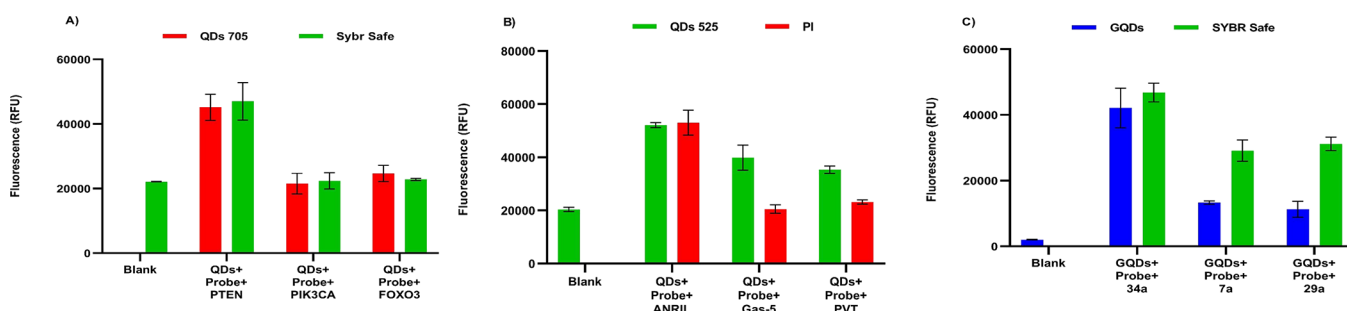


Figure 8. Graph demonstrating the specific binding efficiency of developed nanoconjugates toward specific RNA sequences in comparison to other nonspecific RNAs. (A) QDs 705 specificity toward PTEN, (B) QDs 525 Specificity toward ANRIL, and (C) GQDs specificity toward 34a.

using three QDs (QD-705, QD-525, and GQDs). The developed sensor efficiently detected the target RNAs in isolated and plasma samples. We assume that after appropriate validation, the assay might prove beneficial to characterize and detect aberrant cell-free circulating miRNA-lncRNA-mRNA.

Expression profiling of targeted oligonucleotide probe, i.e., miRNA (34a), lncRNAs (ANRIL), and mRNA (PTEN) (PDF)

■ ASSOCIATED CONTENT

SI Supporting Information

The Supporting Information is available free of charge at <https://pubs.acs.org/doi/10.1021/acsomega.3c05718>.

■ AUTHOR INFORMATION

Corresponding Author

Pradyumna Kumar Mishra – Division of Environmental Biotechnology, Genetics & Molecular Biology, ICMR-National Institute for Research in Environmental Health, Bhopal

462030, India; orcid.org/0000-0002-0795-2819;
Email: pkm_8bh@yahoo.co.uk

Authors

Pooja Ratre – Division of Environmental Biotechnology, Genetics & Molecular Biology, ICMR-National Institute for Research in Environmental Health, Bhopal 462030, India

Nazim Nazeer – Division of Environmental Biotechnology, Genetics & Molecular Biology, ICMR-National Institute for Research in Environmental Health, Bhopal 462030, India

Arpit Bhargava – Division of Environmental Biotechnology, Genetics & Molecular Biology, ICMR-National Institute for Research in Environmental Health, Bhopal 462030, India; Faculty of Science, Ram Krishna Dharmarth Foundation University, Bhopal 462030, India

Suresh Thareja – Department of Pharmaceutical Sciences and Natural Products, Central University of Punjab, Bathinda 151001, India

Rajnarayan Tiwari – Division of Environmental Biotechnology, Genetics & Molecular Biology, ICMR-National Institute for Research in Environmental Health, Bhopal 462030, India

Vinay Singh Raghuwanshi – Division of Environmental Biotechnology, Genetics & Molecular Biology, ICMR-National Institute for Research in Environmental Health, Bhopal 462030, India

Complete contact information is available at:

<https://pubs.acs.org/10.1021/acsomega.3c05718>

Author Contributions

[†]P.R. and N.N. contributed equally.

Notes

The authors declare no competing financial interest.

ACKNOWLEDGMENTS

The authors are thankful to the Indian Council of Medical Research (ICMR), Department of Health Research (DHR), Ministry of Health & Family Welfare (MoHFW), Government of India, New Delhi, for extramural project (DHR-GIA) funding support to the laboratory of Prof. (Dr.) Pradyumna Kumar Mishra.

ABBREVIATIONS:

lncRNAs-long noncoding ribonucleic acids
miRNAs-micro ribonucleic acids
QGDs-graphene quantum dots
NHS-N-hydroxysuccinimide
EDC-1-ethyl-3-(3-(dimethylamino)propyl) carbodiimide
QDs-quantum dots
ID-intercalating dye
PI-propidium iodide
NFW-nuclease free water
LOD-limit of detection
RFU-relative fluorescence unit

REFERENCES

- (1) Liao, J.; Wang, J.; Liu, Y.; Li, J.; Duan, L. Transcriptome sequencing of lncRNA, miRNA, mRNA and interaction network constructing in coronary heart disease. *BMC Medical Genom.* **2019**, *12* (1), 124.
- (2) Gao, C.; Li, H.; Zhuang, J.; Zhang, H.; Wang, K.; Yang, J.; Liu, C.; Liu, L.; Zhou, C.; Sun, C. The construction and analysis of ceRNA networks in invasive breast cancer: a study based on The Cancer Genome Atlas. *Cancer Manag Res.* **2018**, 1–11.

- (3) Bahramy, A.; Zafari, N.; Rajabi, F.; Aghakhani, A.; Jayedi, A.; Khaboushan, A. S.; Zolbin, M. M.; Yekaninejad, M. S. Prognostic and diagnostic values of non-coding RNAs as biomarkers for breast cancer: An umbrella review and pan-cancer analysis. *Front. Mol. Biosci.* **2023**, *10*, 1096524.

- (4) Agrawal, D.; Kumari, R.; Ratre, P.; Rehman, A.; Srivastava, R. K.; Reszka, E.; Goryacheva, I. Y.; Mishra, P. K. Cell-free circulating miRNAs-lncRNAs-mRNAs as predictive markers for breast cancer risk assessment in women exposed to indoor air pollution. *Case Stud. Chem. Environ. Eng.* **2022**, *6*, No. 100267.

- (5) Volovat, S. R.; Volovat, C.; Hordila, I.; Hordila, D.-A.; Mirestean, C. C.; Miron, O. T.; Lungulescu, C.; Scripcariu, D. V.; Stolniceanu, C. R.; Konsoulova-Kirova, A. A. MiRNA and lncRNA as potential biomarkers in triple-negative breast cancer: a review. *Front. Oncol.* **2020**, *10*, No. 526850.

- (6) Fan, C.-N.; Ma, L.; Liu, N. Systematic analysis of lncRNA-miRNA-mRNA competing endogenous RNA network identifies four-lncRNA signature as a prognostic biomarker for breast cancer. *J. Transl. Med.* **2018**, *16* (1), 264.

- (7) Song, X.; Cao, G.; Jing, L.; Lin, S.; Wang, X.; Zhang, J.; Wang, M.; Liu, W.; Lv, C. Analysing the relationship between lnc RNA and protein-coding gene and the role of lnc RNA as ce RNA in pulmonary fibrosis. *J. Cell Mol. Med.* **2014**, *18* (6), 991–1003.

- (8) Zhou, W.; Ye, X.-L.; Xu, J.; Cao, M.-G.; Fang, Z.-Y.; Li, L.-Y.; Guan, G.-H.; Liu, Q.; Qian, Y.-H.; Xie, D. The lncRNA H19 mediates breast cancer cell plasticity during EMT and MET plasticity by differentially sponging miR-200b/c and let-7b. *Sci. Signal.* **2017**, *10* (483), No. eaak9557.

- (9) Ren, Y.; Jia, H.-H.; Xu, Y.-Q.; Zhou, X.; Zhao, X.-H.; Wang, Y.-F.; Song, X.; Zhu, Z.-Y.; Sun, T.; Dou, Y. Paracrine and epigenetic control of CAF-induced metastasis: the role of HOTAIR stimulated by TGF- β 1 secretion. *Mol. Cancer* **2018**, *17*, 5.

- (10) Wilusz, J. E.; Sunwoo, H.; Spector, D. L. Long noncoding RNAs: functional surprises from the RNA world. *Genes Dev.* **2009**, *23* (13), 1494–1504.

- (11) Ratre, P.; Jain, B.; Kumari, R.; Thareja, S.; Tiwari, R.; Srivastava, R. K.; Goryacheva, I. Y.; Mishra, P. K. Bioanalytical applications of graphene quantum dots for circulating cell-free nucleic acids: a review. *ACS Omega* **2022**, *7* (44), 39586–39602.

- (12) Shandilya, R.; Ranjan, S.; Khare, S.; Bhargava, A.; Goryacheva, I. Y.; Mishra, P. K. Point-of-care diagnostics approaches for detection of lung cancer-associated circulating miRNAs. *Drug Discovery Today* **2021**, *26* (6), 1501–1509.

- (13) Ratre, P.; Nazeer, N.; Kumari, R.; Thareja, S.; Jain, B.; Tiwari, R.; Kamthan, A.; Srivastava, R. K.; Mishra, P. K. Carbon-Based Fluorescent Nano-Biosensors for the Detection of Cell-Free Circulating MicroRNAs. *Biosensors* **2023**, *13* (2), 226.

- (14) Chauhan, P.; Bhargava, A.; Kumari, R.; Ratre, P.; Tiwari, R.; Srivastava, R. K.; Goryacheva, I. Y.; Mishra, P. K. Surface-enhanced Raman scattering biosensors for detection of oncomiRs in breast cancer. *Drug Discovery Today* **2022**, *27* (8), 2121–2136.

- (15) Zhang, P.; Zhuo, Y.; Chang, Y.; Yuan, R.; Chai, Y. Electrochemiluminescent graphene quantum dots as a sensing platform: a dual amplification for microRNA assay. *Anal. Chem.* **2015**, *87* (20), 10385–10391.

- (16) Hu, T.; Zhang, L.; Wen, W.; Zhang, X.; Wang, S. Enzyme catalytic amplification of miRNA-155 detection with graphene quantum dot-based electrochemical biosensor. *Biosens. Bioelectron.* **2016**, *77*, 451–456.

- (17) Shandilya, R.; Kumari, R.; Bunkar, N.; Bhargava, A.; Chaudhury, K.; Goryacheva, I. Y.; Mishra, P. K. A photonic dual nano-hybrid assay for detection of cell-free circulating mitochondrial DNA. *J. Pharm. Biomed. Anal.* **2022**, *208*, No. 114441.

- (18) Shandilya, R.; Sobolev, A. M.; Bunkar, N.; Bhargava, A.; Goryacheva, I. Y.; Mishra, P. K. Quantum dot nanoconjugates for immuno-detection of circulating cell-free miRNAs. *Talanta* **2020**, *208*, No. 120486.

- (19) Shandilya, R.; Bunkar, N.; Kumari, R.; Bhargava, A.; Chaudhury, K.; Goryacheva, I. Y.; Mishra, P. K. Immuno-cytometric detection of

circulating cell free methylated DNA, post-translationally modified histones and micro RNAs using semi-conducting nanocrystals. *Talanta* **2021**, *222*, No. 121516.

(20) Shandilya, R.; Kumari, R.; Singh, R. D.; Chouksey, A.; Bhargava, A.; Goryacheva, I. Y.; Mishra, P. K. Gold based nano-photonics approach for point-of-care detection of circulating long non-coding RNAs. *Nanomedicine* **2021**, *36*, No. 102413.

(21) Shandilya, R.; Bhargava, A.; Ratre, P.; Kumari, R.; Tiwari, R.; Chauhan, P.; Mishra, P. K. Graphene quantum-dot-based nano-photonics approach for targeted detection of long noncoding RNAs in circulation. *ACS Omega* **2022**, *7* (30), 26601–26609.

(22) Shandilya, R.; Bhargava, A.; Bunkar, N.; Tiwari, R.; Goryacheva, I. Y.; Mishra, P. K. Nanobiosensors: Point-of-care approaches for cancer diagnostics. *Biosens. Bioelectron.* **2019**, *130*, 147–165.

(23) Kartha, R. V.; Subramanian, S. Competing endogenous RNAs (ceRNAs): new entrants to the intricacies of gene regulation. *Front. Genet.* **2014**, *5*, 8.

(24) Tran, L.; Park, S. Highly sensitive detection of dengue biomarker using streptavidin-conjugated quantum dots. *Sci. Rep.* **2021**, *11* (1), 15196.

(25) Tan, X.; Li, Q.; Yang, J. CdTe QDs based fluorescent sensor for the determination of gallic acid in tea. *Spectrochim. Acta, Part A* **2020**, *224*, No. 117356.

■ NOTE ADDED AFTER ASAP PUBLICATION

This paper published ASAP on October 18, 2023 with an error in the title. The error was corrected and the paper reposted on October 20, 2023.